On Infrasound Waveguides and Dispersion

Petru T. Negraru and Eugene T. Herrin
Southern Methodist University

INTRODUCTION

Waveguides are structures that provide for efficient propagation of waves. One of the earliest applications of a waveguide is the speaking tube, which was used on ships. Propagation in some waveguides leads to dispersion, a phenomenon in which the phase velocity depends on the frequency. Dispersion of elastic and sound waves in solids and liquids has been observed and treated in the scientific literature for a long time (Worzel and Ewing 1948; Pekeris 1948; Ewing *et al.* 1957). However, in the sub-audible acoustic domain, usually referred to as infrasound (frequencies below 20 Hz), dispersion was recognized only recently (Herrin *et al.* 2006). There are reports of dispersed signals recorded on infrasound sensors on the passing of surface waves of large earthquakes (Donn and Posmentier 1964; Cook 1971), but the signals in those instances were the result of ground to air coupling, and the dispersion was not related to sound propagation. In the current paper we derive the dispersion equation of an acoustic waveguide and relate it to infrasound observations.

THEORY

Infrasound propagation is controlled by effective sound speed, which relates the effect of temperature (as a consequence of ideal gas law) and wind strength and direction:

$$V_{eff} = V_T + n \cdot \nu ,$$

where V_{eff} is the effective sound speed, $V_T \oplus 20\sqrt{T}$; T is the Kelvin temperature; and the dot product $n \cdot \nu$ is the component of wind strength in the direction of the propagation. Throughout the paper when we use the term sound velocity (or sound speed) we actually mean effective sound speed, which will have the wind component in it.

The following discussion follows that of Garland (1979). Consider a medium composed of a layer overlain by a half space (Figure 1), separated by an interface, with $\alpha' > \alpha$, where α and α' are the sound velocities in the layer and half space, respectively. The lower boundary is a rigid surface. Complete reflection, where the acoustic waves are trapped in the layer in Figure 1, will occur only if the reflection angle θ at the interface is equal to or greater than the critical angle. The waveguide solution is complicated by the phase change for the supercritical reflections on the interface. At the rigid boundary there is total reflection with no phase change.

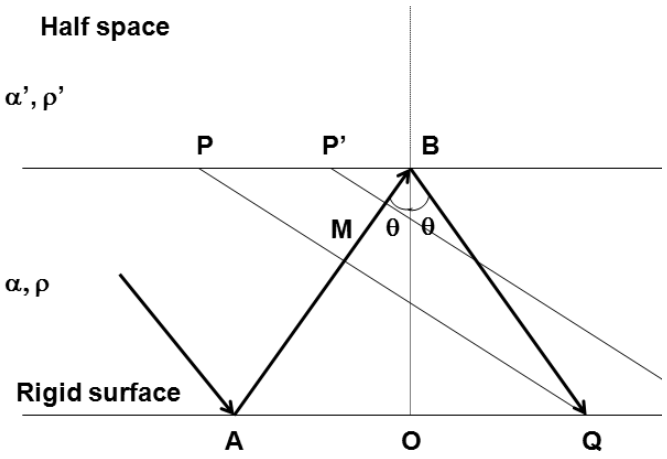

▲ **Figure 1.** Schematic representation of a wave confined to a layer by successive reflections.

Consider an upgoing propagating wave as represented by the wavefronts PQ and $P'Q'$. The wavefronts PQ or $P'Q'$ represent waves traveling upward from A and waves that have traveled the path MBQ and have been reflected at Q. For constructive interference to occur the phase difference between the components of the disturbance at PQ must be $2n\pi$ radians, where $n = 0, 1, 2, 3 \ldots$

Consider a non-zero phase shift at the interface. The phase of the wave that has traveled the extra distance MBQ will be advanced an angle

$$\frac{2\pi}{\lambda_0} MBQ$$

where λ_0 is the true wavelength (in the direction MB, perpendicular on the wavefront) of the interfering waves. After some algebraic manipulation it can be shown that

$$\frac{2\pi}{\lambda_0} MBQ = 2kH\sqrt{\frac{c^2}{\alpha^2} - 1} ,$$

where k is the wavenumber in the x direction, and c, the horizontal phase velocity, is related to the incidence angle by

$$c = \frac{\alpha}{\sin(\theta)} .$$

doi: 10.1785/gssrl.80.4.565

In order to have constructive interference, the total phase shift due to the additional propagation MBQ and the difference in the phase of the upward and downward traveling waves (the z component of the phase) must be equal to $2n\pi$:

$$2kH\sqrt{\frac{c^2}{\alpha^2}-1}-\phi=2n\pi\,.$$

The phase change ϕ due to the supercritical reflections at the interface is (Officer 1958; equation 2-162)

$$\tan\frac{\phi}{2}=\frac{\rho}{\rho'}\sqrt{\frac{\sin^2\theta-\frac{\alpha^2}{\alpha'^2}}{1-\sin^2\theta}}\,.$$

Therefore the expression for the constructive interference (dispersion equation), after making use of the relation $\sin(\theta) = \alpha/c$, becomes:

$$kH\sqrt{\frac{c^2}{\alpha^2}-1}-\tan^{-1}\frac{\rho}{\rho}\sqrt{\frac{\frac{\alpha^2}{c^2}-\frac{c^2}{\alpha^2}}{1-\frac{\alpha^2}{c^2}}}=n\pi$$

where ρ and ρ' are the densities in the layer and half space. This expression is very similar to the dispersion equation for Love waves (Ewing *et al.* 1957) except that the ratio of shear moduli is replaced by the ratio of the densities, and one boundary is rigid rather than a free surface. In the modeling section (see below) we have used this equation to compute a theoretical dispersion curve, which is used to derive the thickness of the ducting layer and the velocity contrast with the confining half space above.

EMPIRICAL OBSERVATIONS

The only observation of dispersed infrasound, up to this manuscript, was reported by Herrin *et al.* (2006), analyzing a signal recorded at an infrasound array in the Republic of Korea. We present here additional dispersed infrasound signals recorded in Trans-Pecos, Texas, in 1997 and in Nevada in 2007.

2005 Korean Signals

Herrin *et al.* (2006) analyzed the signals recorded in Korea. They observed a suite of eight strongly dispersed signals at a small-aperture array located on an island off the northwest coast of South Korea. They used a trial and error forward modeling approach to interpret the signals as waveguides propagating in a low-velocity layer. The frequency of the dispersed signals ranged from 1.8 to 16 Hz. The cut-off frequency of the anti-aliasing filter is 16 Hz. The model had a layer thickness of 80 m. Based on the duration of the signal and the observed phase velocities they estimated a source/receiver distance of 90–100 km. To our knowledge this is the first report in the literature of a dispersed infrasound signal.

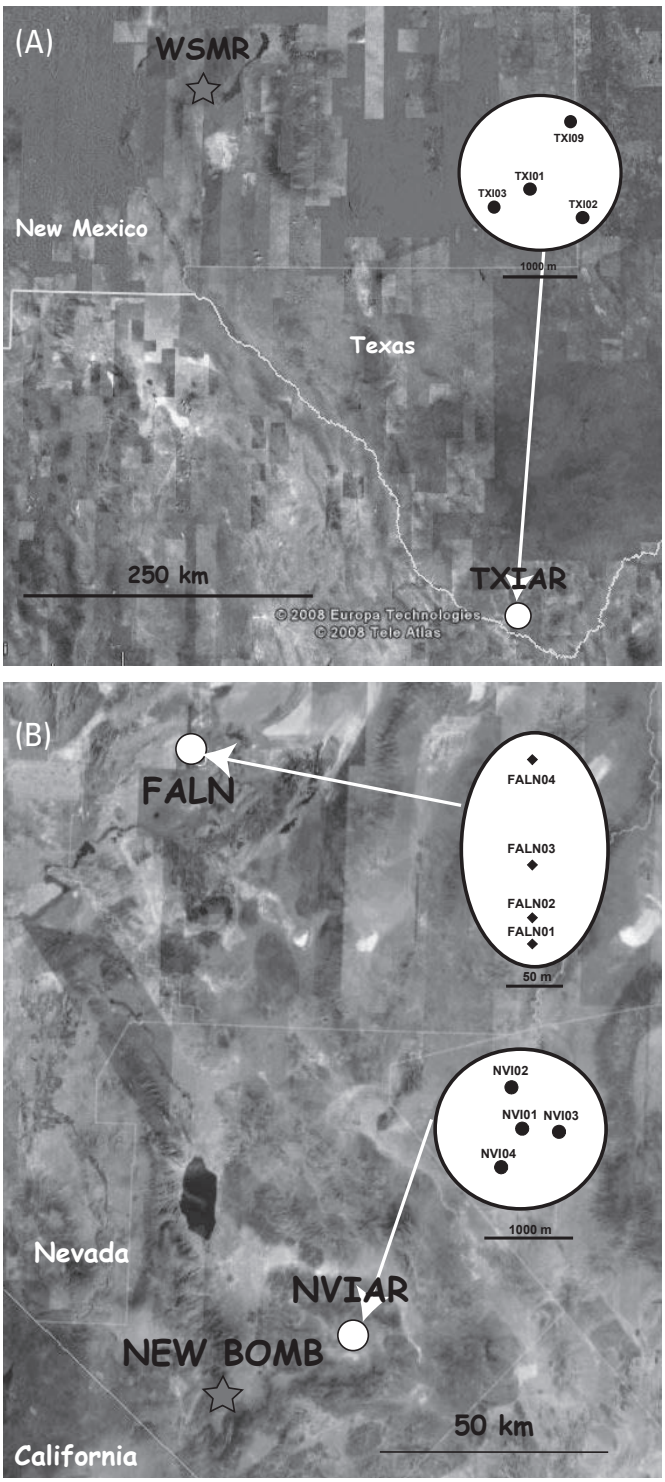

▲ **Figure 2.** (A) Satellite image of the area between the source and array for 1997 signal and (B) 2007 dataset. Also shown are the configurations of each array.

Trans-Pecos, Texas

A dispersed infrasound signal from a surface explosion at White Sands Missile Range was recorded at TXIAR on 19 November 1997. The TXIAR array is located close to the village of Lajitas, TX, in the Big Bend area, at a distance of 546 km from the explosion source. Figure 2 shows the approximate path of the

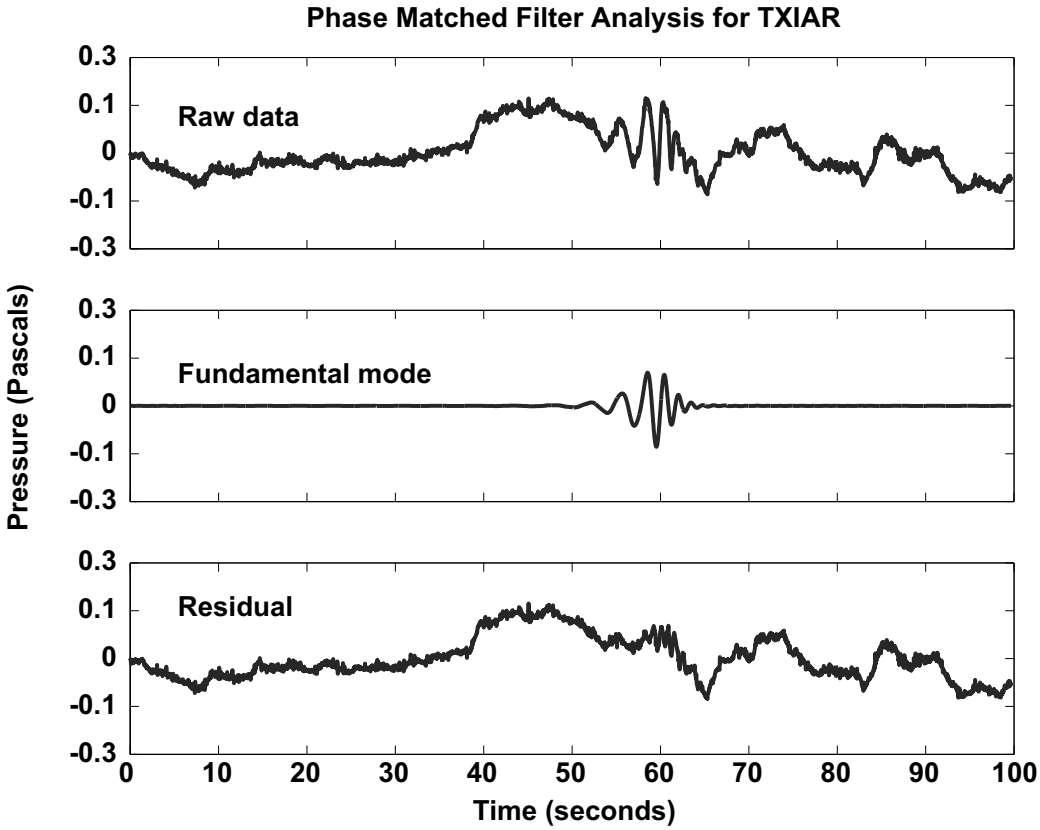

▲ **Figure 3.** Output of the phase-matched filter technique for the TXIAR signal.

signals, while Figure 3 shows the actual signal. Though multiple arrivals were recorded from this event, only the infrasound arrival with a mean travel velocity (total distance divided by the total travel time) of 339 m/s exhibits dispersion. The mean travel velocity (celerity) is used in the infrasound community to provide information about the path of the signal. In our case such a celerity indicates that the signal propagated in the troposphere (Kulichkov *et al.* 2000). The dispersion of this signal ranges from 0.2 to above 1 Hz.

Nevada

During a 2007 experiment designed to understand the propagation of infrasound signals at local and regional distances (up to 300 km from the source), we recorded several dispersed signals at NVIAR and FALN, at distances from the source of 36 km and 157 km, respectively. NVIAR is a permanent array located in the vicinity of the city of Hawthorne, NV, where there is an ammunition disposal facility (New Bomb). The approximate location of the array including configuration is shown in Figure 2. FALN was a temporary array located a few kilometers north of the city of Fallon, NV, deployed for a week in September 2007. The signals for NVIAR and FALN are shown in Figures 4 and 5, respectively. It should be noted that some of the signals recorded at NVIAR have energy arriving about a second before the arrival of the main dispersed wavetrain (Figure 4). We interpret this as a direct wave from the source. We have observed this impulsive early arrival only on NVIAR, which is closest to the source. It appears that this is a random occurrence that depends on the local wind conditions. Because NVIAR was closer to the source, there is energy above the noise level up to 10 Hz, but the dispersion ranges from 1 to 4 Hz, while for FALN, because of the high frequency attenuation, the dispersion range is from 1 to 2 Hz.

Modeling

We extracted the fundamental mode of the signal using the phase-match filter algorithm (Herrin and Goforth 1977), a technique widely used in seismology in the study of surface waves. The phase-matched filters are a class of linear filters in which the Fourier phase of the filter is equal to that of a given signal. The phase-matched filtering starts with a trial dispersion curve obtained either from the envelope functions of the signal filtered with a suite of Gaussian filters (the multiple filter technique of Dziewonski *et al.* 1969) or obtained by an analyst. An iterative process of correlation in the Fourier domain is used to refine the trial dispersion and to extract the desired signal, which in our case is the fundamental mode. The flow diagram of the process is shown in Table 1 of Herrin and Goforth (1977). Figures 3–5 of this paper show the original signal, the fundamental mode, and the residuals for the TXIAR, NVIAR, and FALN arrays. Usually the energy on the residuals is interpreted as being the higher modes of the dispersed waves. However, the signal recorded at NVIAR, shown in Figure 4, exhibits interference between the dispersed signal and a direct wave arrival about 1 s earlier. In this case the residual will contain both the direct arrival and the energy from the higher modes.

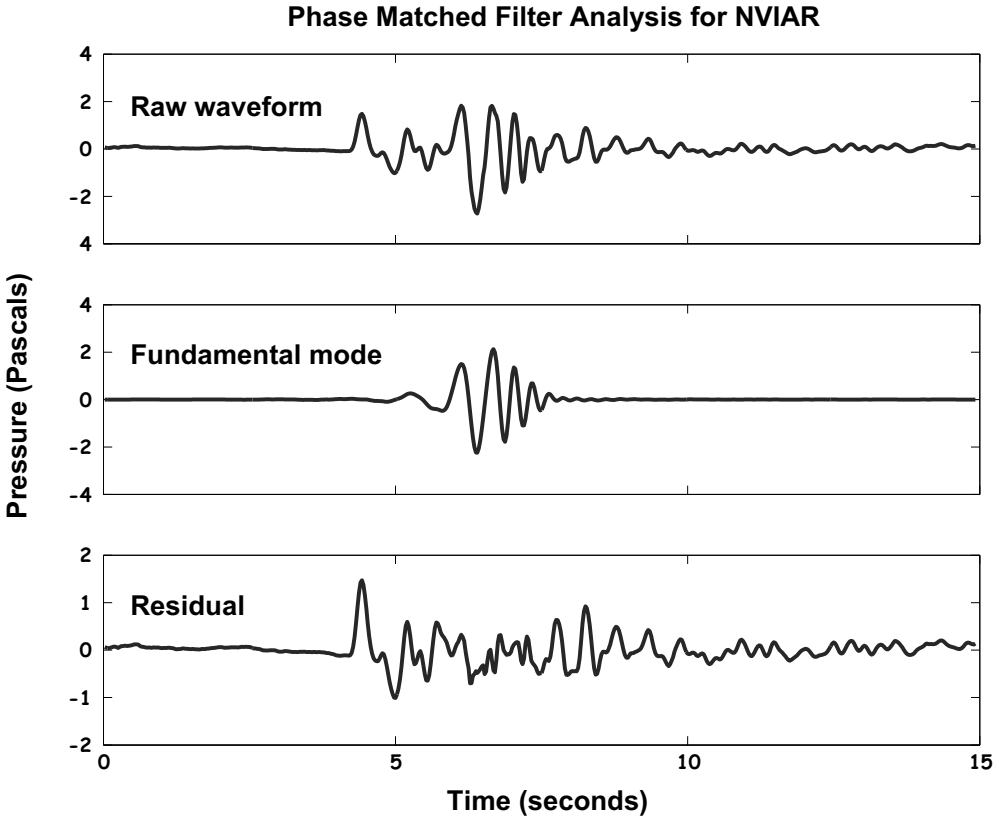

▲ **Figure 4.** Output of the phase-matched technique for NVIAR signals.

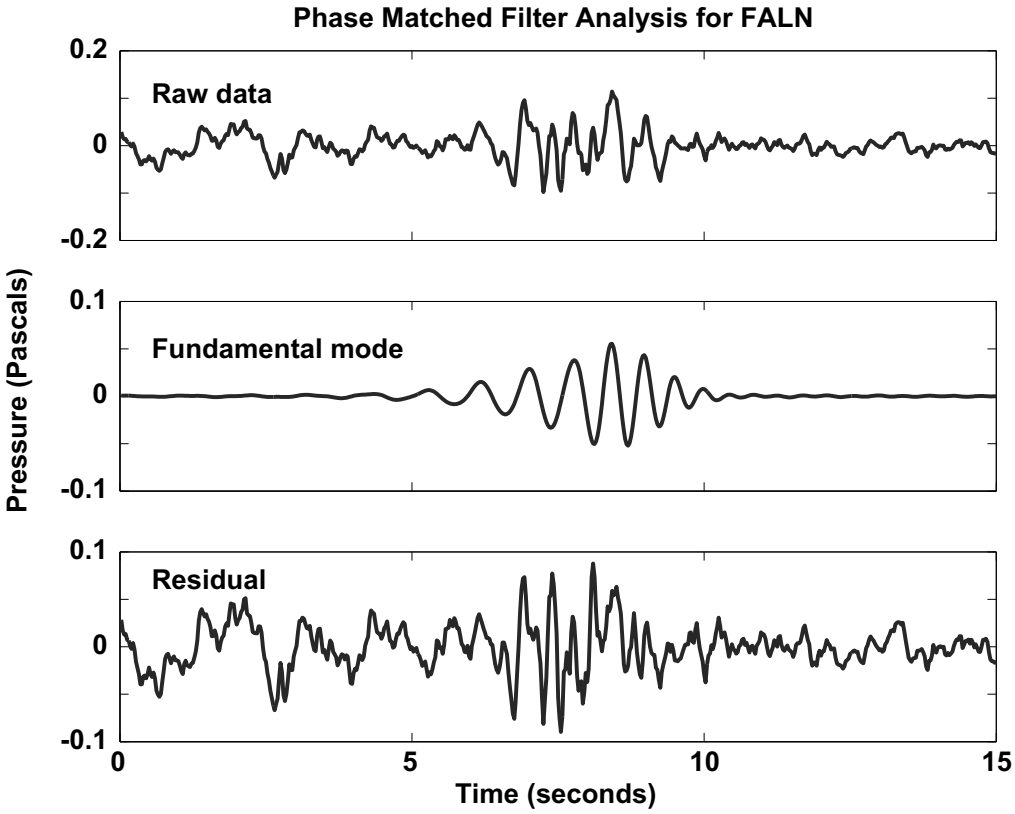

▲ **Figure 5.** Output of the phase-matched technique at FALN.

Once we extracted the fundamental mode, we measured the dispersion from the zero crossing observations. We used the derived dispersion equation to match the observed dispersion with a theoretical model. In the dispersion equation we have $n = 0$ for the fundamental mode and $n = 1$ for the first higher mode. The densities at the observed pressure and temperature conditions can be computed with the approach suggested by Weast 1969. The ratio of densities between the layer and half space is approximately 1.03. Figure 6 shows the observed dispersion for the TXIAR signal and the theoretical dispersion curves for a layer 600 m thick. The velocity in the layer is 335.8 m/s, while the velocity in the half space is 340 m/s. Figure 7 shows the observed dispersion for the NVIAR signals and the theoretical dispersion curve for a layer approximately 80 m thick and velocities of 340 m/s in the layer and 347 m/s in the half space. In Figure 8, which shows the FALN observations, the layer thickness is 120 m and the velocities are 340 m/s and 348 m/s. In all three figures there is a good agreement between the observed and the modeled dispersion curves.

DISCUSSION

In addition to the Korean signal discussed by Herrin *et al.* (2006), we present several other dispersed signals. Also it is important to note that we have ground truth information about the sources. This allowed us to make a link between the phase velocity and celerity. Though multiple arrivals were observed at TXIAR and FALN, only the arrivals with celerity values comparable to the phase velocity exhibit dispersion (Table 1). The later arrivals have celerities below 300 m/s, indicating that they probably propagated through the stratosphere.

The signals presented in this paper are different from the Korean signal discussed by Herrin *et al.* (2006). A comparison among the signals is given in Table 1. The most important difference is the frequency range of the dispersion, which is the main controlling factor on the thickness of the inversion layer, while the velocity difference controls mostly the slope of the dispersion. In consequence the thickness for the inversion layer varies from 80 m for the Korean signals (1.8–16 Hz) to 600 m for the TXIAR signal (0.2–1 Hz). During the 2007 experiment we acquired meteorological data at the Hawthorne airport in the direct path from New Bomb to FALN. The effective sound speed profile reveals an inversion layer approximately 100 m thick, which is also supported by our modeling (80–120 m). The signal with the longest propagation path is TXIAR (546 km), which has the largest inversion layer. The thicker inversion layer is definitely possible in winter, and due to the longer wavelengths, the signals could propagate for longer distances. Figure 9 shows the temperature profile recorded at the Hawthorne airport. The wind data are not shown because they are completely unreliable at these low altitudes. At higher altitudes the wind readings tend to be close to zero, but the readings at the lower altitudes appear to be related to the oscillation of the probe following the release of the balloon. If we translate

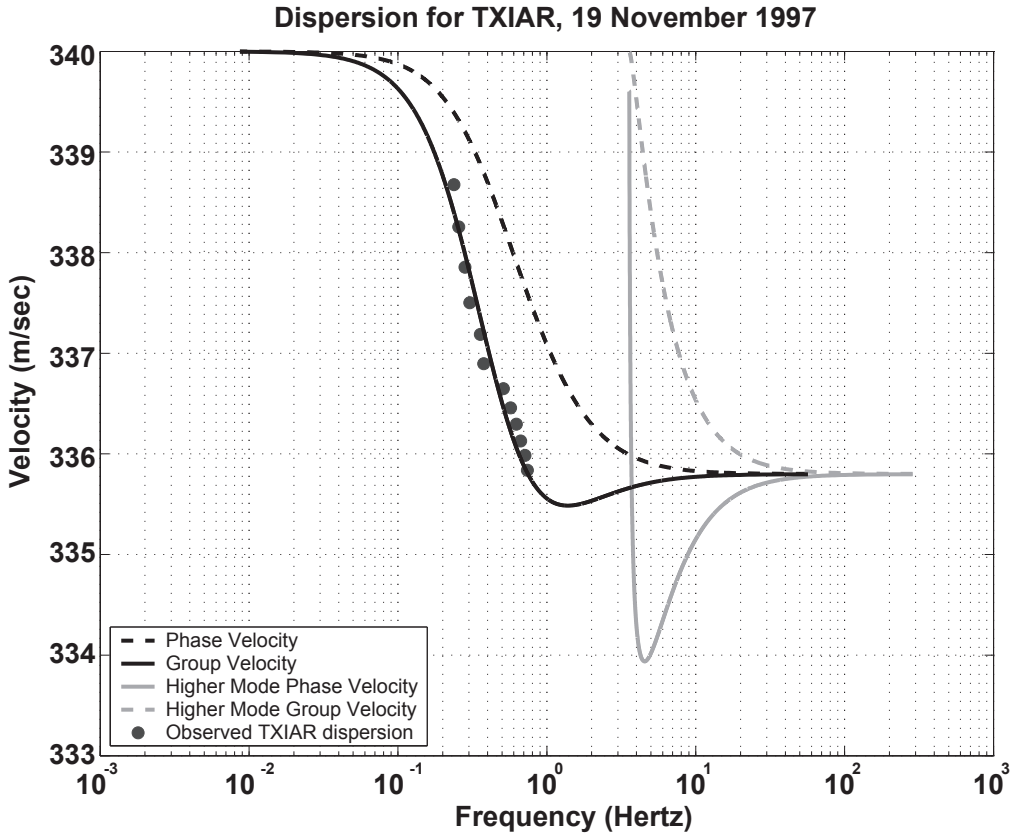

▲ **Figure 6.** Observed and theoretical dispersion curves for the TXIAR signal shown in Figure 3.

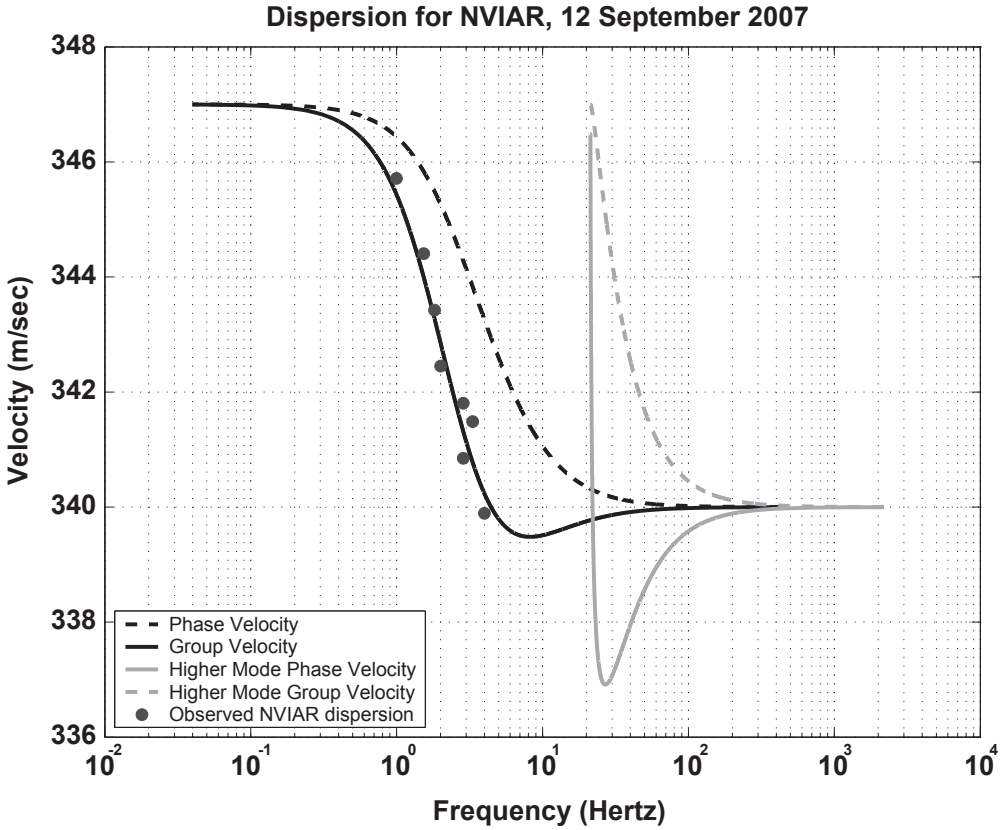

▲ **Figure 7.** Observed and theoretical dispersion curves for the NVIAR signals shown in Figure 4.

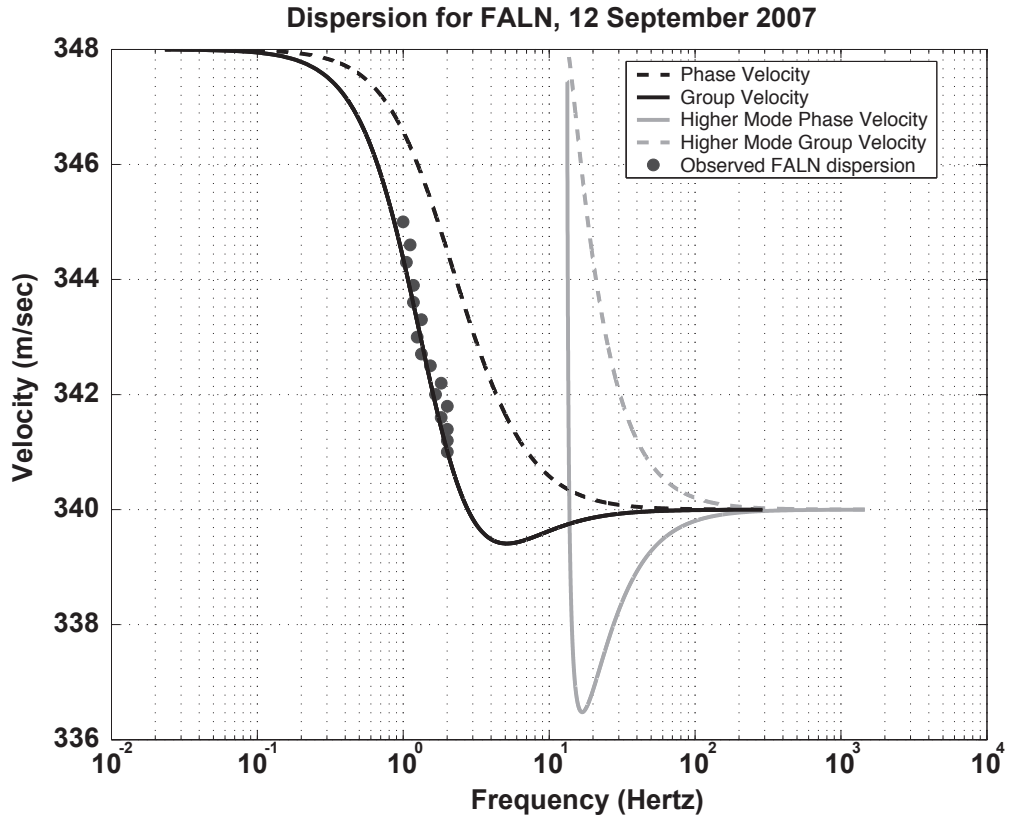

▲ **Figure 8.** Observed and theoretical dispersion curves for the FALN signals shown in Figure 5.

TABLE 1
Comparison of Infrasound Signals with Dispersion.
The phase velocity for TXIAR, NVIAR, and FALN is only for the very first arrival.

	Korea	TXIAR	NVIAR	FALN
Frequency(Hz)	1.8–16	0.2–1	1–4	1–2
Layer thickness (m)	80	600	80	120
Velocity of the layer (m/s)	338	335.8	340	340
Velocity of the half space (m/s)	344	340	347	348
Source/Receiver Distance (km)	90–100	546.2	36	157
Phase velocity (m/s)	338–343	341	354	352
Celerity (m/s)	Not known	339	348	345

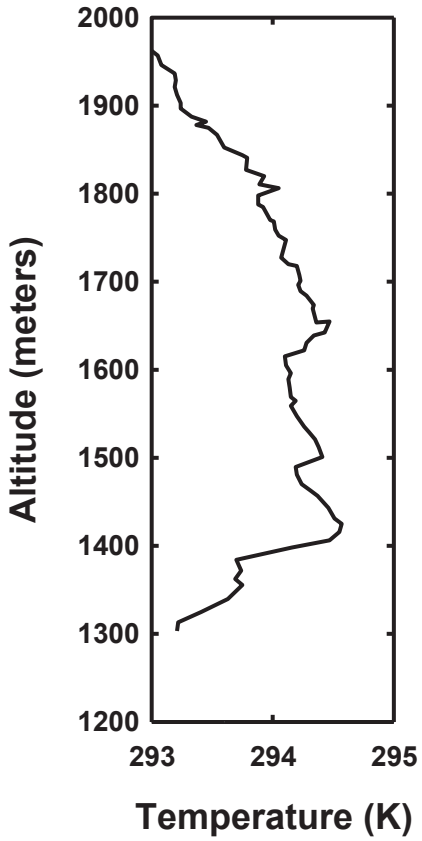

▲ **Figure 9.** Atmospheric model acquired at Hawthorne Airport in Nevada, in the path of the propagating signals.

the sound speed to temperature values, neglecting the wind conditions we obtain a difference in temperature between the layer and half space of approximately 12° C in Nevada, while the temperature data shows only 2° C difference. Therefore the wind must affect the propagation. This conclusion is also supported by the unusual high phase velocities recorded during the Nevada experiment. Future field experiments will focus on characterizing the inversion layer, particularly the boundary between the layer and half space. In any case, this analysis shows that dispersed infrasound signals can be successfully modeled as propagation in waveguides using very simple sound velocity models.

REFERENCES

Cook, R. K. (1971). Infrasound radiated during the Montana earthquake of 1959 August 18. *Geophysical Journal International* **26**, 191–198.

Donn, W. L., and E. S. Posmentier (1964). Ground-coupled air waves from the great Alaskan earthquake. *Journal of Geophysical Research* **69** (24), 5,357–5,361.

Dziewonski, A., S. Bloch, and M. Landisman (1969). A technique for the analysis of transient seismic signals. *Bulletin of the Seismological Society of America* **59**, 427–444.

Ewing, M., W. Jardetzky, and F. Press (1957). *Elastic Waves in Layered Media*. New York: McGraw-Hill Book Company.

Garland, G. D. (1979). *Introduction to Geophysics: Mantle, Core, and Crust*. 2nd ed. Toronto: Saunders.

Herrin, E., T. S. Kim, and B. W. Stump (2006). Evidence for an infrasound waveguide. *Geophysical Research Letters* **33**, L07815; doi: 10.1029/2005GL025492.

Herrin, E. T., and T. Goforth (1977). Phase-matched filters: Application to the study of Rayleigh waves. *Bulletin of the Seismological Society of America* **67**, 1,259–1,275.

Kulichkov, S. N., D. O. ReVelle, R. W. Whitaker, and O. M. Raspopov (2000). On so called "tropospheric" arrivals at the long distances from surface explosions. In *Proceedings of the 9th Annual International Symposium on Long-Range Sound Propagation*, 229–237. NCPA Report No. DM0501-01. National Center for Physical Acoustics.

Officer, C. B (1958). *Introduction to the Theory of Sound Transmission*. New York: McGraw-Hill.

Pekeris, C. L. (1948). Theory of propagation of explosive sound in shallow water. *Geological Society of America Memoir* **27**, 117 pps.

Weast, R. C. (1969). *Handbook of Chemistry and Physics*. 50th ed. Cleveland, OH: The Chemical Rubber Co.

Worzel, J. L., and M. Ewing (1948). Explosion sounds in shallow water. *Geological Society of America Memoir* **27**, 53 pps.

Southern Methodist University
P.O. Box 750395
Dallas, Texas 75206 U.S.A.
pnegraru@smu.edu
(P. T. N.)